Advances in Nano Research, *Vol. 11, No. 5 (2021) 467-477*
https://doi.org/10.12989/anr.2021.11.5.467

Numerical and computational modeling for nonlinear dynamic simulation of curved shells under multi-physical fields

Jing He*[1] and Yu Sun[2]

[1]*Institute for Advanced Studies in Humanities and Social Sciences, Beihang University, Beijing 100000, Beijing, China*
[2]*CIGIS (China) Limited, Beijing 100007, Beijing, China*

(*Received February 17, 2020, Revised August 7, 2021, Accepted August 28, 2021*)

Abstract. This research is devoted to explore the nonlinear vibration characteristics of smart nanoshells under multi-phyisical magneto-electric fields. The nano-scale shell has been treated as a thin shell with prescribed curvature which is modeled by nonlocal elasticity theory. The material composition of the smart nanoshell has been considered as a two phase composite for which the effective properties depend on the percentage of each phase. The discretization of governing equations has been carried out based on differential quadrature method (DQM). It has been exhibited that nonlinear vibration properties of curved nanoshells rely on nonlocality coefficient, piezoelectric phase percentage, radius of curvature, and electrical/magnetic potential.
Keywords: DQM; Magneto-electro-elastic material; nanoshell; nonlinear vibrations; nonlocal theory

1. Introduction

An example for a smart material is piezoelectric-magnetic-elastic material in which magnetic-electrical conditions would result in mechanical deformations (Aboudi 2001, Pan and Han 2005). The above fact is associated with the coupling of magnetic-electric and elastic fields (Li and Shi 2009, Guo *et al*. 2016). In such materials, the material characteristics may be especified from elastic, piezoelectric and magnetic components. Structural components (beams, shells and plates) made of MEE materials have been commonly exploited for actuating and sensing in smart machines. The material distribution in these structures may be homogenous or non-homogenous. By assuming the varying material profiles within the thickness of structures, the material distributions have been considered to be nonhomogenous. As an example, a functional graded material is a non-homogenous material in which two materials are involved and all material properties change from one material to another. In regard to the percentages and volume fractions of each material, the effective properties of the structures may be charactrized. There are several investigations on smart piezoelectric-magnetic-elastic structures having functionally graded distribution (Kumaravel *et al*. 2007).

Many experiments and investigations have been carried out on various materials and structures (Zhao *et al*. 2020, Xu *et al*. 2021, Li *et al*. 2021a, b, Liu *et al*. 2020, 2021, Zhang *et al*. 2016, 2021, Jiang *et al*. 2021, Yang *et al*. 2021). According to recent analysis and nano-scale simulations, it has been stated that the mechanical attributes of nano-sized piezo-electric and piezo-magnetic structures are relied on small scale effects (Barati 2017, Ahmed *et al*. 2019, Al-Maliki *et al*. 2019, Fenjan *et al*. 2019, Mirjavadi *et al*. i, j, k). However, owning to the reason that classical continuum modelling has been identified as a scale-independent approach, studying and exploring the mechanical specifications of a low-dimension structure via classical continuum mechanics gives fallacious results and subsequently incorrect designing. Albeit, the atomistic modelling and molecular simulation are affective approaches for establishing the scale-dependent specifications of low-dimension structures, their utilization is not more reasonable owning to the need for numerous computational efforts. For reducing the computational efforts, a number of scale-dependent mechanical models which include the nonlocal elasticity theory (Eringen 1972), strains gradient elasticity theory, refined couple stresses theory and etc, have been developed for accommodating low-dimension factors by introducing the scale parameters and have been widely employed for studying the mechanical specifications of micro or nano structures (Thai and Vo 2012, Eltaher *et al*. 2012, Akbas 2016, Abdullah *et al*. 2021, Ahmed *et al*. 2020 and 2021, Raheef *et al*. 2021, Fenjan *et al*. 2020a, b, Abdulrazzaq *et al*. 2020, Al-Maliki *et al*. 2020, Hamad *et al*. 2019, Muhammad *et al*. 2019, Shariati *et al*. 2020a, b, Barati and Zenkour 2019a, b, Ebrahimi and Barati a, b, c, d). The intelligent materials introduced in the prior paragraphs have been widely exploited in nano-structures and nano-devices (Ke *et al*. 2014, Liu *et al*. 2018, Ebrahimi and Barati 2019a, b). Furthermore, at the nanoscale, the behaviors of structures are different from macro scale structures. Such behaviors are owning to the inclusion of low-dimension influences. The low-dimension influences have been included in higher-order elasticity theories, for example Eringen's elasticity, which is also applied by other researchers.

The present study is allocated to investigate the

*Corresponding author, Ph.D.,
E-mail: bhhejing@buaa.edu.cn

ISSN: 2287-237X (Print), 2287-2388 (Online)

nonlinear vibration characteristics of smart nanoshells under magneto-electric fields. The nano-scale shell has been treated as a thin shell with prescribed curvature which is modeled by nonlocal elasticity theory. The material composition of the smart nanoshell has been considered as a two phase composite for which the effective properties depend on the percentage of each phase. The discretization of governing equations has been carried out based on differential quadrature method (DQM). It has been exhibited that nonlinear vibration properties of curved nanoshells rely on nonlocality coeffcient, piezoelectric phase percentage, radius of curvature, and electrical/ magnetic potential.

2. Theory of non-local elasticity for piezo-magnetic structures

According to the theory of non-local elasticity for smart magnetic-piezoelectric-elastic materials, stresses σ_{ij} electrical displacements D_i and magnetic inductions B_i can be defined in below form:

$$\sigma_{ij} = \int_V \alpha(|x' - x|, \tau)\,[C_{ijkl}\varepsilon_{kl}(x') - e_{mij}E_m(x') - q_{nij}H_n(x')]dV(x') \quad (1a)$$

$$D_i = \int_V \alpha(|x' - x|, \tau)\,[e_{ikl}\varepsilon_{kl}(x') + s_{im}E_m(x') + d_{in}H_n(x')]dV(x') \quad (1b)$$

$$B_i = \int_V \alpha(|x' - x|, \tau)\,[q_{ikl}\varepsilon_{kl}(x') + d_{im}E_m(x') + \chi_{in}H_n(x')]dV(x') \quad (1c)$$

where V defines the volume. Above relations are associated with strains ε_{kl}, and electric-magnetic field (E_m, H_n). Till to now, mechanical analysis of piezo-magnetic nano-structures is performed based on diverse values for nonlocal parameter. Some of papers used actual value of nonlocal parameter with unit of *nm*, but some papers used normalized values for nonlocal factor in such a way that nonlocal parameter is normalized with respect to the length of nano-structure. Ke *et al*. (2014) and other authors used normalized values for nonlocal parameter as μ = e_0a/L = 0.1~0.3 for studying vibrations of smart nanobeams with length L. Also, all components of stress field, electrical field displacement (D_i) and magnetic induction (B_i) for a scale-dependent shell associated with nonlocal elasticity may be introduced by

$$\sigma_{ij} - (e_0a)^2\nabla^2\sigma_{ij} = C_{ijkl}\varepsilon_{kl} - e_{mij}E_m - q_{nij}H_n \quad (2a)$$

$$D_i - (e_0a)^2\nabla^2 D_i = e_{ikl}\varepsilon_{kl} + s_{im}E_m + d_{in}H_n \quad (2b)$$

$$B_i - (e_0a)^2\nabla^2 B_i = q_{ikl}\varepsilon_{kl} + d_{im}E_m + \chi_{in}H_n \quad (2c)$$

where ∇^2 is the Laplacian operator.

3. MEE composites

A single-curved nanoshell of dimension L and h has been shown in Fig.1. This curved nanoshell is made of a

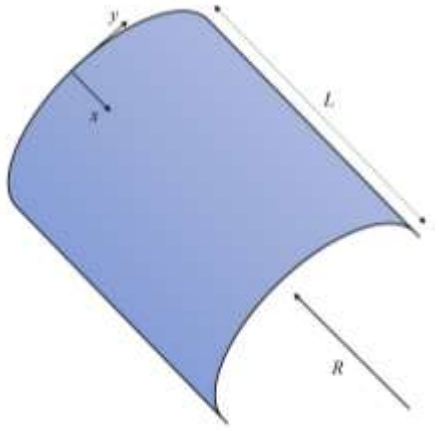

Fig. 1 A single-curved shell

Table 1 Material properties for piezo-magnetic curved shell made of $BaTiO_3$-$CoFe_2O_4$.

Property	V_f = 0	V_f = 0.2	V_f = 0.4	V_f = 0.6	V_f = 0.8
C_{11} (*GPa*)	286	250	225	200	175
C_{13}	170	145	125	110	100
C_{33}	269.5	240	220	190	170
e_{31} (C/m^2)	0	-2	-3	-3.5	-4
e_{33}	0	4	7	11	14
q_{31} (*N/Am*)	580	410	300	200	100
q_{33}	700	550	380	260	120
k_{11} (10^{-9} *C/Vm*)	0.08	0.33	0.8	0.9	1
k_{33}	0.093	2.5	5	7.5	10
d_{11} (10^{-12} *Ns/VC*)	0	2.8	4.8	6	6.8
d_{33}	0	2000	2750	2500	1500
x_{11} (10^{-4} Ns^2/C^2)	-5.9	-3.9	-2.5	-1.5	-0.8
x_{33}	1.57	1.33	1	0.75	0.5
α_1 (10^{-6})	10	11.7	13	14.11	14.98
α_3	10	9.72	9.15	8.37	7.44

MEE composite having two phases: a piezoelectric phase $BaTiO_3$ with volume fraction V_f and a magnetic phase $CoFe_2O_4$. All of material properties for the phases can be found in Table 1 which contains elastic (C_{ij}), piezoelectric (e_{ij}) and piezo-magnetic (q_{ij}) coefficients. Furthermore, k_{ij}, d_{ij} and x_{ij} respectively express dielectric, magnetic-electrical and magnetic permeability coefficients.

4. Single-curvature shell formulation

There are different theories for modeling of plates and shells. By using thin shell theory for a curved nanoshell with curvature R, the three-dimensional displacement field which contains axial (u), circumferential (v) and transverse (w) components can be expressed as follows:

$$d_1(x, y, z) = u(x, y) - z\frac{\partial w}{\partial x}(x, y) \quad (3)$$

$$d_2(x,y,z) = v(x,y) - \frac{z}{R}\frac{\partial w}{\partial y}(x,y) \tag{4}$$

$$d_3(x,y,z) = w(x,y) \tag{5}$$

Above field components result in below relations foe the strain field:

$$\begin{aligned}\varepsilon_{xx} &= \frac{\partial u}{\partial x} - z\frac{\partial^2 w}{\partial x^2} + \frac{1}{2}\left(\frac{\partial w}{\partial x}\right)^2\\ \varepsilon_{yy} &= \frac{\partial v}{\partial y} - \frac{w}{R} - z\frac{\partial^2 w}{\partial y^2} + \frac{1}{2}\left(\frac{\partial w}{\partial y}\right)^2\\ \gamma_{xy} &= \frac{\partial u}{\partial y} + \frac{\partial v}{\partial x} - 2z\frac{\partial^2 w}{\partial x \partial y} + \frac{\partial w}{\partial x}\frac{\partial w}{\partial y}\end{aligned} \tag{6}$$

The induced electro-magnetic field having electric potential (Φ) and magnetic potential (Υ) to the curved nano-scale shell can be expressed as:

$$\Phi(x,y,z) = -cos(\xi z)\phi(x,y) + \frac{2z}{h}V_E \tag{7}$$

$$\Upsilon(x,y,z) = -cos(\xi z)\gamma(x,y) + \frac{2z}{h}\Omega \tag{8}$$

with $\xi = \pi/h$. Next, V_E and Ω define the exterior electrical voltages and magnetic potentials induced to the smart shell. All ingredients of electrical field (E_x, E_y, E_z) and magnet field (H_x, H_y, H_z) can be obtained as:

$$E_x = -\Phi_{,x} = cos(\xi z)\frac{\partial \phi}{\partial x}, \tag{9}$$

$$E_y = -\Phi_{,y} = cos(\xi z)\frac{\partial \phi}{\partial y}, \tag{10}$$

$$E_z = -\Phi_{,z} = -\xi\, sin(\xi z)\phi - \frac{2V}{h} \tag{11}$$

$$H_x = -\Upsilon_{,x} = cos(\xi z)\frac{\partial \gamma}{\partial x}, \tag{12}$$

$$H_y = -\Upsilon_{,y} = cos(\xi z)\frac{\partial \gamma}{\partial y}, \tag{13}$$

$$H_z = -\Upsilon_{,z} = -\xi\, sin(\xi z)\gamma - \frac{2\Omega}{h} \tag{14}$$

Knowing that *ea* is nonlocal parameter, Eq. (2) results in below field components for the curved nano-scale shell containing stain and electro-magnetic field:

$$\begin{aligned}&(1-(ea)^2\nabla^2)\sigma_{xx} = \tilde{C}_{11}\varepsilon_{xx} + \tilde{C}_{12}\varepsilon_{yy}\\ &-\tilde{e}_{31}E_z - \tilde{q}_{31}H_z\end{aligned} \tag{15}$$

$$\begin{aligned}&(1-(ea)^2\nabla^2)\sigma_{yy} = \tilde{C}_{12}\varepsilon_{xx} + \tilde{C}_{11}\varepsilon_{yy}\\ &-\tilde{e}_{31}E_z - \tilde{q}_{31}H_z\end{aligned} \tag{16}$$

$$(1-(ea)^2\nabla^2)\sigma_{xy} = \tilde{C}_{66}\gamma_{xy} \tag{17}$$

$$(1-(ea)^2\nabla^2)D_x = +\tilde{s}_{11}E_x + \tilde{d}_{11}H_x \tag{18}$$

$$(1-(ea)^2\nabla^2)D_y = +\tilde{s}_{11}E_y + \tilde{d}_{11}H_y \tag{19}$$

$$\begin{aligned}&(1-(ea)^2\nabla^2)D_z = \tilde{e}_{31}\varepsilon_{xx} + \tilde{e}_{31}\varepsilon_{yy}\\ &+\tilde{s}_{33}E_z + \tilde{d}_{33}H_z\end{aligned} \tag{20}$$

$$(1-(ea)^2\nabla^2)B_x = +\tilde{d}_{11}E_x + \tilde{\chi}_{11}H_x \tag{21}$$

$$(1-(ea)^2\nabla^2)B_y = +\tilde{d}_{11}E_y + \tilde{\chi}_{11}H_y \tag{22}$$

$$\begin{aligned}&(1-(ea)^2\nabla^2)B_z = \tilde{q}_{31}\varepsilon_{xx} + \tilde{q}_{31}\varepsilon_{yy}\\ &+\tilde{d}_{33}E_z + \tilde{\chi}_{33}H_z\end{aligned} \tag{23}$$

Reduced forms the constants C_{ij}, e_{ij} and q_{ij} can be found in the paper of Mirjavadi *et al*. (2020). Five governing equations for the curved MEE nanoshell can be expressed as:

$$\frac{\partial N_{xx}}{\partial x} + \frac{\partial N_{xy}}{\partial y} = I_0\frac{\partial^2 u}{\partial t^2} - I_1\frac{\partial^3 w}{\partial x \partial t^2} \tag{24}$$

$$\frac{\partial N_{xy}}{\partial x} + \frac{\partial N_{yy}}{\partial y} = I_0\frac{\partial^2 v}{\partial t^2} - I_1\frac{\partial^3 w}{\partial y \partial t^2} \tag{25}$$

$$\begin{aligned}&\frac{\partial^2 M_{xx}}{\partial x^2} + 2\frac{\partial^2 M_{xy}}{\partial x \partial y} + \frac{\partial^2 M_{yy}}{\partial y^2} + \frac{N_{xx}}{R}\\ &+(N_{x0}+N_{xx})\left(\frac{\partial^2 w}{\partial x^2}\right) + (N_{y0}+N_{yy})\left(\frac{\partial^2 w}{\partial y^2}\right)\\ &+2N_{xy}\frac{\partial^2 w}{\partial x \partial y} = +I_0\frac{\partial^2 w}{\partial t^2} + I_1\frac{\partial^3 u}{\partial x \partial t^2} + I_1\frac{\partial^3 v}{\partial y \partial t^2}\\ &-I_2\left(\frac{\partial^4 w}{\partial x^2 \partial t^2} + \frac{\partial^4 w}{\partial y^2 \partial t^2}\right)\end{aligned} \tag{26}$$

$$\int_{-h/2}^{h/2}\begin{pmatrix}cos(\xi z)\dfrac{\partial D_x}{\partial x} + cos(\xi z)\dfrac{\partial D_y}{\partial y}\\ +\xi\, sin(\xi z)D_z\end{pmatrix}dz = 0 \tag{27}$$

$$\int_{-h/2}^{h/2}\begin{pmatrix}cos(\xi z)\dfrac{\partial B_x}{\partial x} + cos(\xi z)\dfrac{\partial B_y}{\partial y}\\ +\xi\, sin(\xi z)B_z\end{pmatrix}dz = 0 \tag{28}$$

where $\{I_0, I_1, I_2\} = \int_{-h/2}^{h/2}\rho\{1, z, z^2\}dz$ are mass inertias. Also, note that N_{ij} and M_{ij} (ij = xx, xy, yy) describe membrane forces and bending moments:

$$\begin{aligned}N_{xx} &= \int_{-h/2}^{h/2}(\sigma_{xx})dz\\ N_{xy} &= \int_{-h/2}^{h/2}(\sigma_{xy})dz\\ N_{yy} &= \int_{-h/2}^{h/2}(\sigma_{yy})dz\\ M_{xx} &= \int_{-h/2}^{h/2}z(\sigma_{xx})dz\\ M_y &= \int_{-h/2}^{h/2}z(\sigma_{yy})dz\\ M_{xy} &= \int_{-h/2}^{h/2}z(\sigma_{xy})dz\end{aligned} \tag{29}$$

Herein, this is supposed that the MEE nano-sized shell is affected by outer electrical voltages and magnetic potentials. Accordingly, N_{x0}, N_{y0} define the in-plane loading owning to external electrical voltages V, magnetic

potentials Ω are defined as:

$$\begin{aligned} N_{x0} &= N_{y0} = N^E + N^H \\ N^E &= -\int_{-h/2}^{h/2} \tilde{e}_{31} \frac{2V_E}{h} dz\,, \\ N^H &= -\int_{-h/2}^{h/2} \tilde{q}_{31} \frac{2\Omega}{h} dz \end{aligned} \tag{30}$$

Based upon Hamilton's rule, it is feasible to express correlated edge conditions for MEE nano-scale shell based upon n_x and n_y as cosines of directions:

$$u = 0, or N_{xx} n_x + N_{xy} n_y = 0 \tag{31}$$

$$v = 0, or N_{xy} n_x + N_{yy} n_y = 0 \tag{32}$$

$$\begin{aligned} &w = 0, or n_x \left(\frac{\partial M_{xx}}{\partial x} + \frac{\partial M_{xy}}{\partial y} - N_{x0} \frac{\partial w}{\partial x}\right) \\ &+ n_y \left(\frac{\partial M_{yy}}{\partial y} + \frac{\partial M_{xy}}{\partial x} - N_{y0} \frac{\partial w}{\partial y}\right) = 0 \end{aligned} \tag{33}$$

$$\frac{\partial w}{\partial x} = 0, or M_{xx} n_x + M_{xy} n_y = 0 \tag{34}$$

$$\frac{\partial w}{\partial y} = 0, or M_{xy} n_x + M_{yy} n_y = 0 \tag{35}$$

$$\begin{aligned} &\phi = 0, \\ &or \int_{-h/2}^{h/2} \left(cos(\xi z) D_x n_x + cos(\xi z) D_y n_y\right) dz = 0 \end{aligned} \tag{36}$$

$$\begin{aligned} &\gamma = 0, \\ &or \int_{-h/2}^{h/2} \left(cos(\xi z) B_x n_x + cos(\xi z) B_y n_y\right) dz = 0 \end{aligned} \tag{37}$$

Determining the integrals represented in Eq. (29) gives the below equations for MEE nano-size shells in the context of nonlocal theory as:

$$\begin{aligned} &(1 - (ea)^2 \nabla^2) N_{xx} = A_{11} \left(\frac{\partial u}{\partial x} + \frac{1}{2} \left(\frac{\partial w}{\partial x}\right)^2\right) \\ &- B_{11} \frac{\partial^2 w}{\partial x^2} + A_{12} \left(\frac{\partial v}{\partial y} - \frac{w}{R} + \frac{1}{2} \left(\frac{\partial w}{\partial y}\right)^2\right) \\ &- B_{12} \frac{\partial^2 w}{\partial y^2} + A_{31}^e \phi + A_{31}^m \gamma \end{aligned} \tag{38}$$

$$\begin{aligned} &(1 - (ea)^2 \nabla^2) M_{xx} = B_{11} \left(\frac{\partial u}{\partial x} + \frac{1}{2} \left(\frac{\partial w}{\partial x}\right)^2\right) \\ &- D_{11} \frac{\partial^2 w}{\partial x^2} + B_{12} \left(\frac{\partial v}{\partial y} - \frac{w}{R} + \frac{1}{2} \left(\frac{\partial w}{\partial y}\right)^2\right) \\ &- D_{12} \frac{\partial^2 w}{\partial y^2} + E_{31}^e \phi + E_{31}^m \gamma \end{aligned} \tag{39}$$

$$\begin{aligned} &(1 - (ea)^2 \nabla^2) N_{yy} = A_{12} \left(\frac{\partial u}{\partial x} + \frac{1}{2} \left(\frac{\partial w}{\partial x}\right)^2\right) \\ &- B_{12} \frac{\partial^2 w}{\partial x^2} + A_{11} \left(\frac{\partial v}{\partial y} - \frac{w}{R} + \frac{1}{2} \left(\frac{\partial w}{\partial y}\right)^2\right) \\ &- B_{11} \frac{\partial^2 w}{\partial y^2} + A_{31}^e \phi + A_{31}^m \gamma \end{aligned} \tag{40}$$

$$\begin{aligned} &(1 - (ea)^2 \nabla^2) M_{yy} = B_{12} \left(\frac{\partial u}{\partial x} + \frac{1}{2} \left(\frac{\partial w}{\partial x}\right)^2\right) \\ &- D_{12} \frac{\partial^2 w}{\partial x^2} + B_{11} \left(\frac{\partial v}{\partial y} - \frac{w}{R} + \frac{1}{2} \left(\frac{\partial w}{\partial y}\right)^2\right) \\ &- D_{11} \frac{\partial^2 w}{\partial y^2} + E_{31}^e \phi + E_{31}^m \gamma \end{aligned} \tag{41}$$

$$\begin{aligned} &(1 - (ea)^2 \nabla^2) N_{xy} = A_{66} \left(\frac{\partial u}{\partial y} + \frac{\partial v}{\partial x} + \frac{\partial w}{\partial x} \frac{\partial w}{\partial y}\right) \\ &- 2B_{66} \frac{\partial^2 w}{\partial x \partial y} \end{aligned} \tag{42}$$

$$\begin{aligned} &(1 - (ea)^2 \nabla^2) M_{xy} = B_{66} \left(\frac{\partial u}{\partial y} + \frac{\partial v}{\partial x} + \frac{\partial w}{\partial x} \frac{\partial w}{\partial y}\right) \\ &- 2D_{66} \frac{\partial^2 w}{\partial x \partial y} \end{aligned} \tag{43}$$

$$\begin{aligned} &\int_{-\hbar/2}^{\hbar/2} (1 - (ea)^2 \nabla^2) D_x \, cos(\xi z) dz = + F_{11}^e \frac{\partial \phi}{\partial x} \\ &+ F_{11}^m \frac{\partial \gamma}{\partial x} \end{aligned} \tag{44}$$

$$\begin{aligned} &\int_{-h/2}^{h/2} (1 - (ea)^2 \nabla^2) D_y \, cos(\xi z) dz = + F_{22}^e \frac{\partial \phi}{\partial y} \\ &+ F_{22}^m \frac{\partial \gamma}{\partial y} \end{aligned} \tag{45}$$

$$\begin{aligned} &\int_{-h/2}^{h/2} (1 - (ea)^2 \nabla^2) D_z \xi \, sin(\xi z) dz = A_{31}^e \left(\frac{\partial u}{\partial x}\right. \\ &\left. + \frac{1}{2} \left(\frac{\partial w}{\partial x}\right)^2\right) + A_{31}^e \left(\frac{\partial v}{\partial y} - \frac{w}{R} + \frac{1}{2} \left(\frac{\partial w}{\partial y}\right)^2\right) \\ &- E_{31}^e \left(\frac{\partial^2 w}{\partial x^2} + \frac{\partial^2 w}{\partial y^2}\right) - F_{33}^e \phi - F_{33}^m \gamma \end{aligned} \tag{46}$$

$$\begin{aligned} &\int_{-\hbar/2}^{\hbar/2} (1 - (ea)^2 \nabla^2) B_x \, cos(\xi z) dz = \\ &+ F_{11}^m \frac{\partial \phi}{\partial x} + X_{11}^m \frac{\partial \gamma}{\partial x} \end{aligned} \tag{47}$$

$$\begin{aligned} &\int_{-h/2}^{h/2} (1 - (ea)^2 \nabla^2) B_y \, cos(\xi z) dz = \\ &+ F_{22}^m \frac{\partial \phi}{\partial y} + X_{22}^m \frac{\partial \gamma}{\partial y} \end{aligned} \tag{48}$$

$$\begin{aligned} &\int_{-h/2}^{h/2} (1 - (ea)^2 \nabla^2) B_z \xi \, sin(\xi z) dz \\ &= A_{31}^m \left(\frac{\partial u}{\partial x} + \frac{1}{2} \left(\frac{\partial w}{\partial x}\right)^2\right) + A_{31}^m \left(\frac{\partial v}{\partial y} - \frac{w}{R} + \frac{1}{2} \left(\frac{\partial w}{\partial y}\right)^2\right) \\ &- E_{31}^m \left(\frac{\partial^2 w}{\partial x^2} + \frac{\partial^2 w}{\partial y^2}\right) - F_{33}^m \phi - X_{33}^m \gamma \end{aligned} \tag{49}$$

in which

$$\{A_{11}, B_{11}, D_{11}\} = \int_{-\hbar/2}^{\hbar/2} \tilde{C}_{11} \{1, z, z^2\} dz, \tag{50}$$

$$\{A_{12}, B_{12}, D_{12}\} = \int_{-\hbar/2}^{\hbar/2} \tilde{C}_{12}\{1, z, z^2\}dz, \tag{51}$$

$$\{A_{66}, B_{66}, D_{66}\} = \int_{-\hbar/2}^{\hbar/2} \tilde{C}_{66}\{1, z, z^2\}dz, \tag{52}$$

$$\{A_{31}^e, E_{31}^e\} = \int_{-\hbar/2}^{\hbar/2} \tilde{e}_{31}\xi\, sin(\xi z)\{1, z\}\, dz \tag{53}$$

$$\{A_{31}^m, E_{31}^m\} = \int_{-\hbar/2}^{\hbar/2} \tilde{q}_{31}\xi\, sin(\xi z)\{1, z\}\, dz \tag{54}$$

$$\{F_{11}^e, F_{22}^e, F_{33}^e\} = \int_{-\hbar/2}^{\hbar/2} \{\tilde{s}_{11}\, cos^2(\xi z), \tilde{s}_{22}\, cos^2(\xi z), \tilde{s}_{33}\xi^2\, sin^2(\xi z)\}\, dz \tag{55}$$

$$\{F_{11}^m, F_{22}^m, F_{33}^m\} = \int_{-\hbar/2}^{\hbar/2} \{\tilde{d}_{11}\, cos^2(\xi z), \tilde{d}_{22}\, cos^2(\xi z), \tilde{d}_{33}\xi^2\, sin^2(\xi z)\}\, dz \tag{56}$$

$$\{X_{11}^m, X_{22}^m, X_{33}^m\} = \int_{-\hbar/2}^{\hbar/2} \{\tilde{\chi}_{11}\, cos^2(\xi z), \tilde{\chi}_{22}\, cos^2(\xi z), \tilde{\chi}_{33}\xi^2\, sin^2(\xi z)\}\, dz \tag{57}$$

The governing equations of thin MEE curved nano-size shell based upon the displacement components and potential components might be determined with the insertion of Eqs. (38)-(49) into Eqs. (24)-(28) as:

$$\begin{aligned}
&A_{11}(\frac{\partial^2 u}{\partial x^2} + \frac{\partial^2 w}{\partial x^2}\frac{\partial w}{\partial x}) - B_{11}\frac{\partial^3 w}{\partial x^3}\\
&+A_{12}(\frac{\partial^2 v}{\partial x \partial y} - \frac{1}{R}\frac{\partial w}{\partial x} + \frac{\partial^2 w}{\partial x \partial y}\frac{\partial w}{\partial y}) - B_{12}\frac{\partial^3 w}{\partial x \partial y^2}\\
&+A_{66}(\frac{\partial^2 u}{\partial y^2} + \frac{\partial^2 v}{\partial x \partial y} + \frac{\partial^2 w}{\partial x \partial y}\frac{\partial w}{\partial y} + \frac{\partial w}{\partial x}\frac{\partial^2 w}{\partial y^2})\\
&-2B_{66}\frac{\partial^3 w}{\partial x \partial y^2} + A_{31}^e\frac{\partial \phi}{\partial x} + A_{31}^m\frac{\partial \gamma}{\partial x}\\
&= (1 - (ea)^2\nabla^2)[I_0\frac{\partial^2 u}{\partial t^2} - I_1\frac{\partial^3 w}{\partial x \partial t^2}]
\end{aligned} \tag{58}$$

$$\begin{aligned}
&A_{66}(\frac{\partial^2 u}{\partial x \partial y} + \frac{\partial^2 v}{\partial x^2} + \frac{\partial^2 w}{\partial x^2}\frac{\partial w}{\partial y} + \frac{\partial w}{\partial x}\frac{\partial^2 w}{\partial x \partial y})\\
&-2B_{66}\frac{\partial^3 w}{\partial x^2 \partial y} + A_{12}(\frac{\partial^2 u}{\partial x \partial y} + \frac{\partial w}{\partial x}\frac{\partial^2 w}{\partial x \partial y})\\
&-B_{12}\frac{\partial^3 w}{\partial x^2 \partial y} + A_{11}(\frac{\partial^2 v}{\partial y^2} - \frac{1}{R}\frac{\partial w}{\partial y} + \frac{\partial^2 w}{\partial y^2}\frac{\partial w}{\partial y})\\
&-B_{11}\frac{\partial^3 w}{\partial y^3} + A_{31}^e\frac{\partial \phi}{\partial y} + A_{31}^m\frac{\partial \gamma}{\partial y}\\
&= (1 - (ea)^2\nabla^2)[I_0\frac{\partial^2 v}{\partial t^2} - I_1\frac{\partial^3 w}{\partial y \partial t^2}]
\end{aligned} \tag{59}$$

$$\begin{aligned}
&B_{11}(\frac{\partial^3 u}{\partial x^3} + \frac{\partial^3 w}{\partial x^3}\frac{\partial w}{\partial x} + \frac{\partial^2 w}{\partial x^2}\frac{\partial^2 w}{\partial x^2})\\
&-D_{11}\frac{\partial^4 w}{\partial x^4} - 2D_{12}\frac{\partial^4 w}{\partial x^2 \partial y^2} - 4D_{66}\frac{\partial^4 w}{\partial x^2 \partial y^2}\\
&-D_{11}\frac{\partial^4 w}{\partial y^4} + B_{12}(\frac{\partial^3 v}{\partial x^2 \partial y} - \frac{1}{R}\frac{\partial^2 w}{\partial x^2}\\
&+\frac{\partial^3 w}{\partial x^2 \partial y}\frac{\partial w}{\partial y} + \frac{\partial^2 w}{\partial x \partial y}\frac{\partial^2 w}{\partial x \partial y}) + 2B_{66}(\frac{\partial^3 u}{\partial x \partial y^2}\\
&+\frac{\partial^3 v}{\partial x^2 \partial y} + \frac{\partial^2 w}{\partial x^2}\frac{\partial^2 w}{\partial y^2} + \frac{\partial w}{\partial x}\frac{\partial^3 w}{\partial x \partial y^2}\\
&+\frac{\partial^3 w}{\partial x^2 \partial y}\frac{\partial w}{\partial y} + \frac{\partial^2 w}{\partial x \partial y}\frac{\partial^2 w}{\partial x \partial y})\\
&+B_{12}(\frac{\partial^3 u}{\partial x \partial y^2} + \frac{\partial w}{\partial x}\frac{\partial^3 w}{\partial x \partial y^2}\\
&+\frac{\partial^2 w}{\partial x \partial y}\frac{\partial^2 w}{\partial x \partial y}) + B_{11}(\frac{\partial^3 v}{\partial y^3}\\
&+\frac{\partial^3 w}{\partial y^3}\frac{\partial w}{\partial y} + \frac{\partial^2 w}{\partial y^2}\frac{\partial^2 w}{\partial y^2})\\
&+\frac{A_{12}}{R}(\frac{\partial u}{\partial x} + \frac{1}{2}(\frac{\partial w}{\partial x})^2) - \frac{B_{12}}{R}\frac{\partial^2 w}{\partial x^2}\\
&+\frac{A_{11}}{R}(\frac{\partial v}{\partial y} - \frac{w}{\alpha} + \frac{1}{2}(\frac{\partial w}{\partial y})^2) - \frac{B_{11}}{R}\frac{\partial^2 w}{\partial y^2}\\
&+E_{31}^e(\frac{\partial^2 \phi}{\partial x^2} + \frac{\partial^2 \phi}{\partial y^2}) + E_{31}^m(\frac{\partial^2 \gamma}{\partial x^2} + \frac{\partial^2 \gamma}{\partial y^2})\\
&+\frac{A_{31}^e}{\alpha}\phi + \frac{A_{31}^m}{\alpha}\gamma + \frac{A_{31}^e}{R}\phi + \frac{A_{31}^m}{R}\gamma\\
&+(1 - (ea)^2\nabla^2)(A_{11}(\frac{\partial u}{\partial x} + \frac{1}{2}(\frac{\partial w}{\partial x})^2)\\
&-B_{11}\frac{\partial^2 w}{\partial x^2} + A_{12}(\frac{\partial v}{\partial y} - \frac{w}{R} + \frac{1}{2}(\frac{\partial w}{\partial y})^2)\\
&-B_{12}\frac{\partial^2 w}{\partial y^2}) + A_{31}^e\phi + A_{31}^m\gamma)(\frac{\partial^2 w}{\partial x^2})\\
&+2(1 - (ea)^2\nabla^2)(A_{66}(\frac{\partial u}{\partial y} + \frac{\partial v}{\partial x} + \frac{\partial w}{\partial x}\frac{\partial w}{\partial y})\\
&-2B_{66}\frac{\partial^2 w}{\partial x \partial y})(\frac{\partial^2 w}{\partial x \partial y}) + (1 - (ea)^2\nabla^2)(A_{12}(\frac{\partial u}{\partial x}\\
&+\frac{1}{2}(\frac{\partial w}{\partial x})^2) - B_{12}\frac{\partial^2 w}{\partial x^2}\\
&+A_{11}(\frac{\partial v}{\partial y} - \frac{w}{R} + \frac{1}{2}(\frac{\partial w}{\partial y})^2)\\
&-B_{11}\frac{\partial^2 w}{\partial y^2} + A_{31}^e\phi + A_{31}^m\gamma)(\frac{\partial^2 w}{\partial y^2})\\
&+(1 - (ea)^2\nabla^2)[-(N^E + N^H)(\frac{\partial^2 w}{\partial x^2} + \frac{\partial^2 w}{\partial y^2})]\\
&= (1 - (ea)^2\nabla^2)[+I_0\frac{\partial^2 w}{\partial t^2}\\
&+I_1\frac{\partial^3 u}{\partial x \partial t^2} + I_1\frac{\partial^3 v}{\partial y \partial t^2} - I_2(\frac{\partial^4 w}{\partial x^2 \partial t^2} + \frac{\partial^4 w}{\partial y^2 \partial t^2})]
\end{aligned}$$

$$\begin{aligned}
&+F_{11}^e\frac{\partial^2 \phi}{\partial x^2} + F_{11}^m\frac{\partial^2 \gamma}{\partial x^2} + F_{22}^e\frac{\partial^2 \phi}{\partial y^2} + F_{22}^m\frac{\partial^2 \gamma}{\partial y^2}\\
&+A_{31}^e(\frac{\partial u}{\partial x} - \frac{w}{R} + \frac{1}{2}(\frac{\partial w}{\partial x})^2 + \frac{\partial v}{\partial y} - \frac{w}{\alpha} + \frac{1}{2}(\frac{\partial w}{\partial y})^2)\\
&-E_{31}^e(\frac{\partial^2 w}{\partial x^2} + \frac{\partial^2 w}{\partial y^2}) - F_{33}^e\phi - F_{33}^m\gamma = 0
\end{aligned} \tag{61}$$

$$\begin{aligned}
&+F_{11}^m\frac{\partial^2 \phi}{\partial x^2} + X_{11}^m\frac{\partial^2 \gamma}{\partial x^2} + F_{22}^m\frac{\partial^2 \phi}{\partial y^2} + X_{22}^m\frac{\partial^2 \gamma}{\partial y^2}\\
&+A_{31}^m(\frac{\partial u}{\partial x} - \frac{w}{R} + \frac{1}{2}(\frac{\partial w}{\partial x})^2 + \frac{\partial v}{\partial y} - \frac{w}{\alpha} + \frac{1}{2}(\frac{\partial w}{\partial y})^2)\\
&-E_{31}^m(\frac{\partial^2 w}{\partial x^2} + \frac{\partial^2 w}{\partial y^2}) - F_{33}^m\phi - X_{33}^m\gamma = 0
\end{aligned} \tag{62}$$

5. Solution by differential quadrature method (DQM)

In the present chapter, differential quadrature method (DQM) has been utilized for solving the governing equations for the MEE nanoshell. According to DQM, at an assumed grid point (x_i, y_j) the derivatives for function F are supposed as weighted linear summation of all functional values within the computation domains as:

$$\frac{d^n F}{dx^n}\Big|_{x=x_i} = \sum_{j=1}^{N} c_{ij}^{(n)} F(x_j) \tag{63}$$

where

$$C_{ij}^{(1)} = \frac{\pi(x_i)}{(x_i - x_j)\,\pi(x_j)} \qquad i,j = 1,2,\dots,N, \qquad i \neq j \tag{64}$$

in which $\pi(x_i)$ is defined by

$$\pi(x_i) = \prod_{j=1}^{N} (x_i - x_j), \quad i \neq j \tag{65}$$

And when $i = j$

$$\begin{aligned} &C_{ij}^{(1)} = c_{ii}^{(1)} = -\sum_{k=1}^{N} C_{ik}^{(1)}, \\ &i = 1,2,\dots,N, \quad i \neq k, \qquad i = j \end{aligned} \tag{66}$$

Then, weighting coefficients for high orders derivatives may be expressed by:

$$\begin{aligned} C_{ij}^{(2)} &= \sum_{k=1}^{N} C_{ik}^{(1)} C_{kj}^{(1)} \\ C_{ij}^{(3)} &= \sum_{k=1}^{N} C_{ik}^{(1)} C_{kj}^{(2)} = \sum_{k=1}^{N} C_{ik}^{(2)} C_{kj}^{(1)} \\ C_{ij}^{(4)} &= \sum_{k=1}^{N} C_{ik}^{(1)} C_{kj}^{(3)} = \sum_{k=1}^{N} C_{ik}^{(3)} C_{kj}^{(1)} \quad i,j = 1,2,\dots,N. \\ C_{ij}^{(5)} &= \sum_{k=1}^{N} C_{ik}^{(1)} C_{kj}^{(4)} = \sum_{k=1}^{N} C_{ik}^{(4)} C_{kj}^{(1)} \\ C_{ij}^{(6)} &= \sum_{k=1}^{N} C_{ik}^{(1)} C_{kj}^{(5)} = \sum_{k=1}^{N} C_{ik}^{(5)} C_{kj}^{(1)} \end{aligned} \tag{67}$$

According to presented approach, the dispersions of grid points based upon Gauss-Chebyshev-Lobatto assumption are expressed as:

$$\begin{aligned} x_i &= \frac{L}{2}\left[1 - \cos\left(\frac{i-1}{N-1}\pi\right)\right] \qquad i = 1,2,\dots,N, \\ y_j &= \frac{b}{2}\left[1 - \cos\left(\frac{j-1}{M-1}\pi\right)\right] \qquad j = 1,2,\dots,M, \end{aligned} \tag{68}$$

Next, the displacement components may be re-written by

$$\begin{aligned} &\{u, v, w, \phi, \gamma\}(x, y) \\ &= \{U, V, W, \Phi, \Upsilon\}(x, y) e^{i\omega_n t} dz \end{aligned} \tag{69}$$

where $\{U, V, W, \Phi, \Upsilon\}$ are the amplitudes. Then, it is possible to express obtained boundary conditions as:

$$\begin{aligned} &\phi = \gamma = w = 0, \\ &\frac{\partial^2 w}{\partial x^2} = \frac{\partial^2 w}{\partial y^2} = 0 \; dz \end{aligned} \tag{70}$$

Now, one can express the modified weighting coefficients for all edges simply-supported as:

$$\begin{aligned} \bar{C}_{1,j}^{(2)} &= \bar{C}_{N,j}^{(2)} = 0, \qquad i = 1,2,\dots,M, \\ \bar{C}_{i,1}^{(2)} &= \bar{C}_{1,M}^{(2)} = 0, \qquad i = 1,2,\dots,N. \end{aligned} \tag{71}$$

And

$$\begin{aligned} \bar{C}_{ij}^{(3)} &= \sum_{k=1}^{N} C_{ik}^{(1)} \bar{C}_{kj}^{(2)} \\ \bar{C}_{ij}^{(4)} &= \sum_{k=1}^{N} C_{ik}^{(1)} \bar{C}_{kj}^{(3)} \end{aligned} \tag{72}$$

Considering DQ solution and including displacements represented in Eq. (69) into Eqs. (58)-(62) yields the following ordinary nonlinear governing equations as:

$$\begin{aligned} &k_{11}U + k_{21}V + k_{31}W + n_1 W^2 + k_{41}\Phi \\ &+ k_{51}\Upsilon = 0 \end{aligned} \tag{73}$$

$$\begin{aligned} &k_{12}U + k_{22}V + k_{32}W + n_2 W^2 + k_{42}\Phi \\ &+ k_{52}\Upsilon = 0 \end{aligned} \tag{74}$$

$$\begin{aligned} &k_{13}U + k_{23}V + k_{33}W + n_3 W^2 + n_4 W^3 \\ &+ n_5 UW + n_6 VW + k_{43}\Phi + k_{53}\Upsilon \\ &+ n_9 \Phi W + n_{10}\Upsilon W + M\ddot{W} = 0 \end{aligned} \tag{75}$$

$$\begin{aligned} &k_{14}U + k_{24}V + k_{34}W + n_7 W^2 + k_{44}\Phi \\ &+ k_{54}\Upsilon = 0 \end{aligned} \tag{76}$$

$$\begin{aligned} &k_{15}U + k_{25}V + k_{35}W + n_8 W^2 + k_{45}\Phi \\ &+ k_{55}\Upsilon = 0 \end{aligned} \tag{77}$$

It must be expressed that n_i and k_{ij} display the components of stiffness matrix respectively in non-linear and linear forms. Owning to this deduction that there are 5 governing equations which are coupled together, providing the closed-form of non-linear stability load as a function of shell deflection (W) is too hard. Thus, by simultaneous solve of Eqs. (73), (74), (76) and (77), it is feasible to calculate displacements (U, V, Φ, Υ) as as functions of shell deflection (W). Next, calculated amplitudes ($\widehat{U}$, $\widehat{V}$, $\widehat{\Phi}, \widehat{\Upsilon}$) have been placed in Eq. (75) in order to determine only one nonlinear equation for the curved shell as

$$\begin{aligned} &k_{13}\widehat{U} + k_{23}\widehat{V} + k_{33}W + n_3 W^2 + n_4 W^3 \\ &+ n_5 \widehat{U}W + n_6 \widehat{V}W + k_{43}\widehat{\Phi} + k_{53}\widehat{\Upsilon} \\ &+ n_9 \widehat{\Phi}W + n_{10}\widehat{\Upsilon}W + M\ddot{W} = 0 \end{aligned} \tag{78}$$

By simplifying the obtained equation, the above equation may be obtained as:

$$\ddot{W} + \frac{K_1}{M}W + \frac{K_2}{M}W|W| + \frac{K_3}{M}W^3 = 0 \tag{79}$$

It must be pointed out that K_1, K_2 and K_3 have complex

forms and expressing their closed forms is very difficult. According to the primary conditions $W = \bar{W}, \dot{W} = 0$at t=0, the solution of Eq. (79) may be assumed with the use of trigonometric function as:

$$W = \bar{W}\, cos(\, \omega_{NL} t) \tag{80}$$

where ω_{NL} exhibits the nonlinear vibration frequency. Finally, the nonlinear vibrational frequency can be expressed by:

$$\omega_{NL} = \sqrt{\frac{K_1}{M} + \frac{8\bar{W}}{3\pi}\frac{K_2}{M} + \frac{3}{4}\frac{K_3}{M}(\bar{W})^2} \tag{81}$$

To present obtained results, non-dimension frequency and deflection can be defined by:

$$\varpi = 10\omega_{NL} L\sqrt{\frac{\rho}{C_{11}}}, \mu = \frac{ea}{a},, \widetilde{W} = \frac{\bar{W}}{h} \tag{82}$$

6. Results and discussions

In this chapter, impacts of different factors such as magneto-electrical field, nonlocality, curvature radius and material compositions on nonlinear vibrational frequencies of curved piezo-magnetic nanoshells have been examined. The thickness of nano-sized shell has been chosen to be h = 1 nm. For the confirmation purpose, nonlinear vibrational frequencies have been compared with those of piezo-magnetic cylindrical nanoshell presented by Ke *et al.* (2014) and a worthy agreement is found according to the findings represented in Table 2.

Fig. 2 illustrates the alteration of normalized non-linear frequencies of single-curve nanoshell versus non-dimensional deflection, for variant nonlocal factors when V_E = 0 and V_f = 20%. One may deduce that non-linear vibrational frequencies of nonlocal single-curve MEE nano-sized shell are always lower than that of local macro-sized shells. Non-linear frequencies decrease via the growing of the nonlocal factor at a fixed magnetic intensity and electrical voltage. This incident is associated with the proof that the low-dimension traces, that characterize the reciprocal affections of every points inside the region, might decline the rigidity of the nano-scaled structures.

In Figs. 3 and 4, changing of non-linear vibrational frequencies of single-curve nanoshell versus non-dimensional deflection is illustrated for variant electrical voltages and magnetic potentials when a = 40h and μ = 0.2. One may deduce that non-linear vibrational frequencies of single-curve MEE nano-dimension shell have been outstandingly impressed by the values and sign of magnetic and electrical potentials for every magnitude of normalized deflections. One may conclude that negative sign of magnetic potentials render lower vibrational frequencies than positive sign intensity factor. While, lower values for electric potential render larger non-linear frequencies. Actually, the inflicted negative/positive magnetic intensities might produce the membrane compressive and tensile loads.

Table 2 Validating the vibrational frequency of a nonlocal magnetic shell

	μ = 0.02		μ = 0.03	
	Ke *et al.* (2014)	present	Ke *et al.* (2014)	present
L/R = 30	0.1657	0.1659	0.1435	0.1438
L/R = 40	0.1296	0.1298	0.1062	0.1067
L/R = 50	0.1114	0.1117	0.0874	0.0879

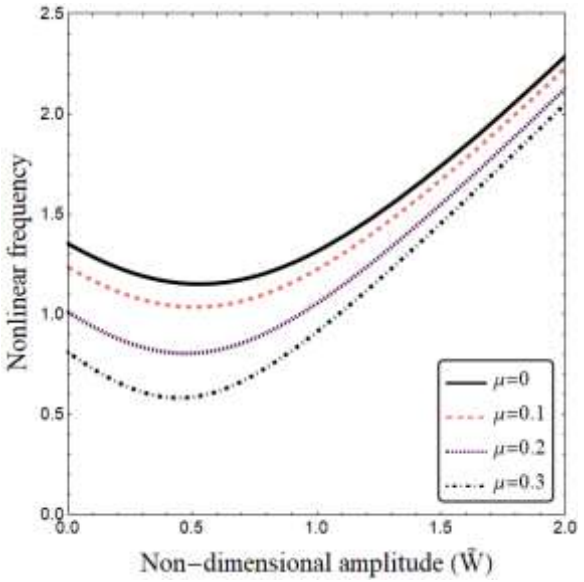

Fig. 2 Changing of non-linear frequency with non-dimensional amplitude against variant nonlocality coefficients (L = 40h, R = 5L, Ω = 0, V_f = 20%)

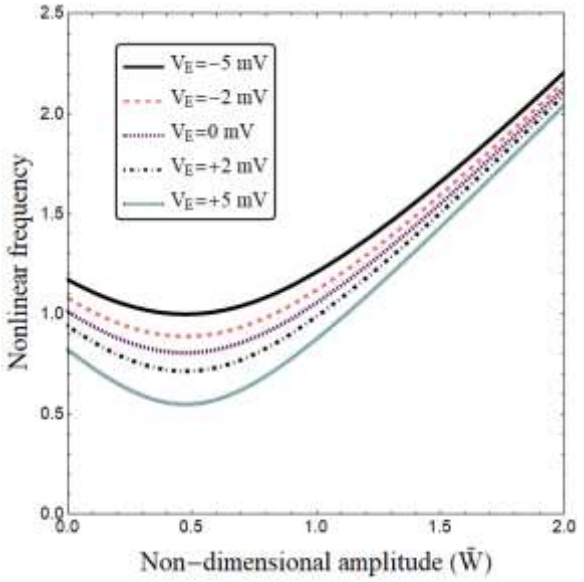

Fig. 3 Changing of non-linear frequency with non-dimensional amplitude against variant electrical voltages (L = 40h, R = 5L, Ω = 0, V_f = 20%)

Whereas, electrical fields show an opposite influence. It is also found that the vibration frequency begins to decline with the increase of non-dimension amplitude. Next, the

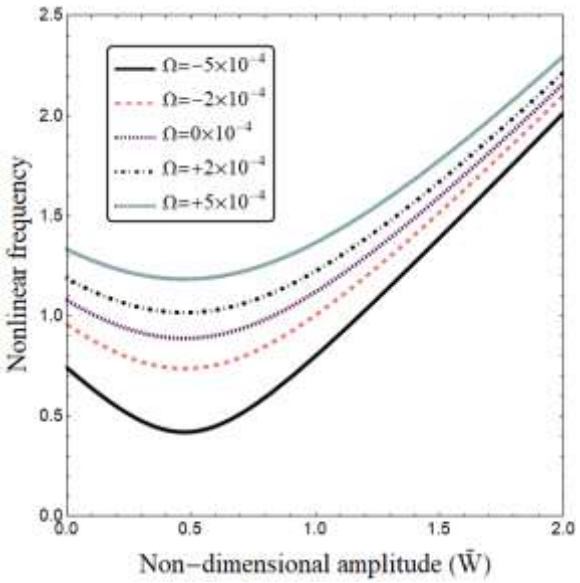

Fig. 4 Changing of non-linear frequency with non-dimensional amplitude against variant magnetic potential (L = 40h, R = 5L, V_E = 0, V_f = 20%)

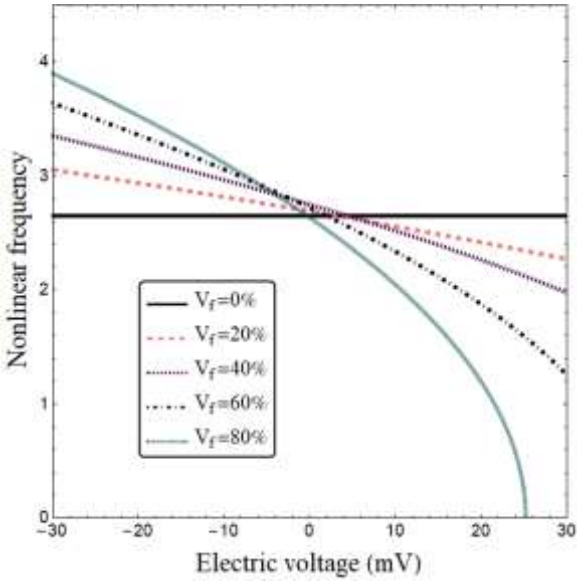

Fig. 5 Changing of non-linear frequency with electrical voltage against variant percentages of piezoelectric phase (R = 5L, μ = 0.2, Ω = 0, W/h = 2)

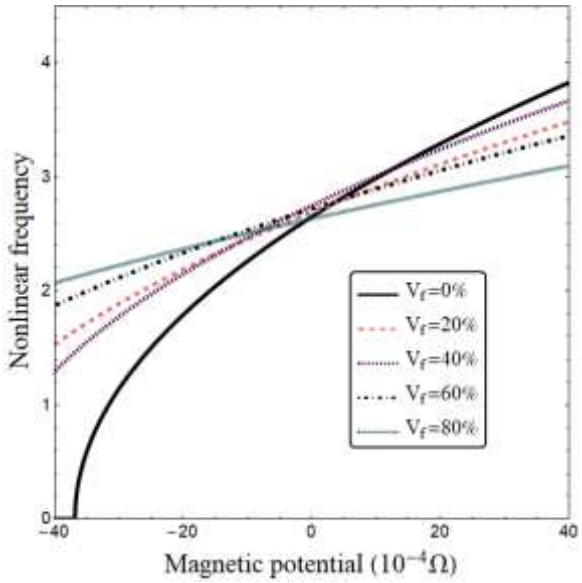

Fig. 6 Changing of non-linear frequency with magnetic potential against variant percentages of piezoelectric phase (R = 5L, μ = 0.2, V_E = 0, W/h = 2)

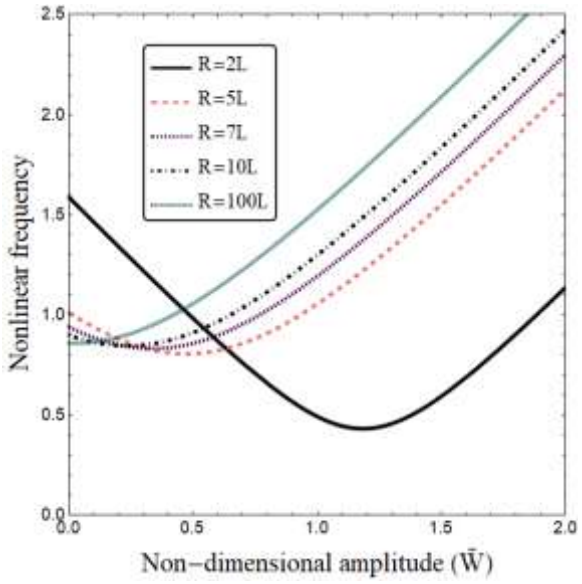

Fig. 7 Changing of non-linear frequency with non-dimensional amplitude against variant curvature radius (R = 5L V_f = 20%, V_E = 0, Ω = 0)

vibration frequency start to rise at greater amounts for non-normalize deflection.

Fig. 5 exhibits vibration frequency changes with respect to electrical voltage taking into consideration differing percentage for piezoelectric ingredient (V_f = 0, 20%, 40%, 60% and 80%). For ease of calculations, the nonlocality coefficient has been chosen to be μ = 0.2. The range of applied voltage has been selected from V_E = -30 mV to V_E = +30 mV. Within the considered electric voltages, it is understood that the vibrational frequencies have decreasing trends. At particular values of positive voltages, the vibrational frequency is zero because of the fact that a positive voltage induces compressive in-plane load to the nano-size shell resulting in lower structural stiffness. For these values of electric voltage, the nano-size shell has buckled and the frequency value is zero.

Non-linear frequency changes with respect to magnetic potential (Ω) taking into consideration differing percentage of piezoelectric ingredient have been exhibited in Fig. 6. For ease of calculation, the nonlocality coefficient has been chosen to be μ = 0.2. The changing of magnetic potential has been selected from Ω = -40× 10^{-4} to Ω = +40× 10^{-4}. Within this range of magnetic potential, it is understood that the vibrational frequencies have augmenting trends. At particular values of negative magnetic potential, the vibrational frequencies are zero and buckling of the nano-size shell happens. The most serious observation from this plot is that non-linear frequencies are growing with less

notable rates as the phase volume grows. Such finding is because at larger amounts of phase volume the nano-size shell is less susceptible to magnetic fields.

Vibrational frequency against normalized deflection of the nano-size shell accounting for differing curvature radius has been exhibited in Fig.7. Note that an infinite curvature radius results in frequency curves for flat plates. So, as the value of curvature has been reduced, the curvature radius has more announced effect on frequency curves.

7. Conclusions

Vibration characteristics of a piezo-magnetic nanoshell with single curvature were reported in the present article. The complete formulation and solution for the problem based on thin shell model was presented. There was no change in vibration frequency versus applied voltage when the piezoelectric volume fraction was zero. Also, applying positive or negative magnetic potentials led to increasing or reducing the vibration frequency. Also, inducing positive or negative magnetic potentials led to increasing or reducing the non-linear frequency. Also, one could report that the vibrational behaviors of the nano-dimension shell are sensitive to ingredients volume. Another observation was that size effects due to nonlocality changed significantly the vibration behaviors of piezo-magnetic nano-sized shell. Also, the dependency of vibration frequency on negative and positive voltages was clearly explained. Also, as the values of radius decline, the radius has more remarkable impression on frequency-deflection plots.

References

Abdullah, W.N., Khalaf, B.S., Ahmed, R.A., Fenjan, R.M. and Faleh, N.M. (2021), "Thermal effects on dynamic response of GOP-Reinforced beams under blast load", *Adv. Concrete Constr.*, **12**(3), 167-174. https://doi.org/10.12989/acc.2021.12.3.167.

Abdulrazzaq, M.A., Muhammad, A.K., Kadhim, Z.D. and Faleh, N.M. (2020), "Vibration analysis of nonlocal strain gradient porous FG composite plates coupled by visco-elastic foundation based on DQM", *Coupled Syst. Mech.*, **9**(3), 201-217. https://doi.org/10.12989/csm.2020.9.3.201.

Aboudi, J. (2001), "Micromechanical analysis of fully coupled electro-magneto-thermo-elastic multiphase composites," *Smart Mater. Struct.*, **10**(5), 867. https://doi.org/10.1088/0964-1726/10/5/303.

Ahmed, R.A., Fenjan, R.M. and Faleh, N.M. (2019), "Analyzing post-buckling behavior of continuously graded FG nanobeams with geometrical imperfections", *Geomech. Eng.*, **17**(2), 175-180. https://doi.org/10.12989/gae.2019.17.2.175.

Ahmed, R.A., Fenjan, R.M., Hamad, L.B. and Faleh, N.M. (2020), "A review of effects of partial dynamic loading on dynamic response of nonlocal functionally graded material beams", *Adv. Mater. Res.*, **9**(1), 33-48. https://doi.org/10.12989/amr.2020.9.1.033.

Ahmed, R.A., Khalaf, B.S., Raheef, K.M., Fenjan, R.M. and Faleh, N.M. (2021), "Investigating dynamic response of nonlocal functionally graded porous piezoelectric plates in thermal environment", *Steel Compos. Struct.*, **40**(2), 243-254. https://doi.org/10.12989/scs.2021.40.2.243.

Akbaş, Ş.D. (2016), "Forced vibration analysis of viscoelastic nanobeams embedded in an elastic medium", *Smart Struct. Syst.*, **18**(6), 1125-1143. http://doi.org/10.12989/sss.2016.18.6.1125.

Al-Maliki, A.F., Faleh, N.M. and Alasadi, A.A. (2019), "Finite element formulation and vibration of nonlocal refined metal foam beams with symmetric and non-symmetric porosities", *Struct. Monit. Maint.*, **6**(2), 147-159. https://doi.org/10.12989/smm.2019.6.2.147.

Al-Maliki, A.F., Ahmed, R.A., Moustafa, N.M. and Faleh, N.M. (2020), "Finite element based modeling and thermal dynamic analysis of functionally graded graphene reinforced beams", *Adv. Comput. Des.*, **5**(2), 177-193. https://doi.org/10.12989/acd.2020.5.2.177.

Barati, M.R. (2017), "Coupled effects of electrical polarization-strain gradient on vibration behavior of double-layered flexoelectric nanoplates", *Smart Struct. Syst.*, **20**(5), 573-581. https://doi.org/10.12989/sss.2017.20.5.573.

Barati, M.R. and Zenkour, A.M. (2019a), "Thermal post-buckling analysis of closed circuit flexoelectric nanobeams with surface effects and geometrical imperfection", *Mech. Adv. Mater. Struct.*, **26**(17), 1482-1490. https://doi.org/10.1080/15376494.2018.1432821.

Barati, M.R. and Zenkour, A. (2019b), "Investigating instability regions of harmonically loaded refined shear deformable inhomogeneous nanoplates", *Iran. J. Sci. Technol. T. Mech. Eng.*, **43**(3), 393-404. https://doi.org/10.1007/s40997-018-0215-4.

Ebrahimi, F. and Barati, M.R. (2018a), "Axial magnetic field effects on dynamic characteristics of embedded multiphase nanocrystalline nanobeams", *Microsyst. Technol.*, **24**(8), 3521-3536. https://doi.org/10.1007/s00542-018-3771-z.

Ebrahimi, F. and Barati, M.R. (2018b), "Damping vibration analysis of graphene sheets on viscoelastic medium incorporating hygro-thermal effects employing nonlocal strain gradient theory", *Compos. Struct.*, **185**, 241-253. https://doi.org/10.1016/j.compstruct.2017.10.021.

Ebrahimi, F. and Barati, M.R. (2018c), "Surface and flexoelectricity effects on size-dependent thermal stability analysis of smart piezoelectric nanoplates", *Struct. Eng. Mech.*, **67**(2), 143-153. https://doi.org/10.12989/sem.2018.67.2.143.

Ebrahimi, F. and Barati, M.R. (2018d), "A nonlocal strain gradient refined plate model for thermal vibration analysis of embedded graphene sheets via DQM", *Struct. Eng. Mech.*, **66**(6), 693-701. https://doi.org/10.12989/sem.2018.66.6.693.

Ebrahimi, F. and Barati, M.R. (2019a), "Hygrothermal effects on static stability of embedded single-layer graphene sheets based on nonlocal strain gradient elasticity theory", *J. Therm. Stress*, **42**(12), 1535-1550. https://doi.org/10.1080/01495739.2019.1662352.

Ebrahimi, F. and Barati, M.R. (2019b), "Damping Vibration Behavior of Viscoelastic Porous Nanocrystalline Nanobeams Incorporating Nonlocal–Couple Stress and Surface Energy Effects", *Iran. J. Sci. Technol. T. Mech. Eng.*, **43**(2), 187-203. https://doi.org/10.1007/s40997-017-0127-8.

Ebrahimi, F. and Barati, M.R. (2020), "Propagation of waves in nonlocal porous multi-phase nanocrystalline nanobeams under longitudinal magnetic field", *Wave Random Complex*, **30**(2), 308-327. https://doi.org/10.1080/17455030.2018.1506596.

Eltaher, M.A., Emam, S.A. and Mahmoud, F.F. (2012), "Free vibration analysis of functionally graded size-dependent nanobeams", *Appl. Math. Comput.*, **218**(14), 7406-7420. https://doi.org/10.1016/j.amc.2011.12.090.

Eringen, A.C. (1972), "Linear theory of nonlocal elasticity and dispersion of plane waves", *Int. J. Eng. Sci.*, **10**(5), 425-435. https://doi.org/10.1016/0020-7225(72)90050-X.

Fenjan, R.M., Ahmed, R.A., Alasadi, A.A. and Faleh, N.M. (2019), "Nonlocal strain gradient thermal vibration analysis of

double-coupled metal foam plate system with uniform and non-uniform porosities", *Coupled Syst. Mech.*, **8**(3), 247-257. https://doi.org/10.12989/csm.2019.8.3.247.

Fenjan, R.M., Hamad, L.B. and Faleh, N.M. (2020a), "Mechanical-hygro-thermal vibrations of functionally graded porous plates with nonlocal and strain gradient effects", *Adv. Aircraft Spacecraft Sci.*, **7**(2), 169-186. https://doi.org/10.12989/aas.2020.7.2.169.

Fenjan, R.M., Ahmed, R.A., Hamad, L.B. and Faleh, N.M. (2020b), "A review of numerical approach for dynamic response of strain gradient metal foam shells under constant velocity moving loads", *Adv. Comput. Des.*, **5**(4), 349-362. https://doi.org/10.12989/acd.2020.5.4.349.

Guo, J., Chen, J. and Pan, E. (2016), "Static deformation of anisotropic layered magnetoelectroelastic plates based on modified couple-stress theory", *Compos. Part B Eng.*, **107**, 84-96. https://doi.org/10.1016/j.compositesb.2016.09.044.

Hamad, L.B., Khalaf, B.S. and Faleh, N.M. (2019), "Analysis of static and dynamic characteristics of strain gradient shell structures made of porous nano-crystalline materials", *Adv. Mater. Res.*, **8**(3), 179-96. https://doi.org/10.12989/amr.2019.8.3.179.

Jiang, L., Wang, Y., Wang, X., Ning, F., Wen, S., Zhou, Y. and Zhou, F.L. (2021), "Electrohydrodynamic printing of a dielectric elastomer actuator and its application in tunable lenses", *Compos. Part A Appl. S.*, **147**, 106461. https://doi.org/10.1016/j.compositesa.2021.106461.

Ke, L.L., Wang, Y.S., Yang, J. and Kitipornchai, S. (2014), "The size-dependent vibration of embedded magneto-electro-elastic cylindrical nanoshells", *Smart Mater. Struct.*, **23**(12), 125036. https://doi.org/10.1088/0964-1726/23/12/125036.

Kumaravel, A., Ganesan, N. and Sethuraman, R. (2007), "Buckling and vibration analysis of layered and multiphase magneto-electro-elastic beam under thermal environment", *Multidiscip. Model. Mater. Struct.*, **3**(4), 461-476. https://doi.org/10.1163/157361107782106401.

Li, Y. and Shi, Z. (2009), "Free vibration of a functionally graded piezoelectric beam via state-space based differential quadrature", *Compos. Struct.*, **87**(3), 257-264. https://doi.org/10.1016/j.compstruct.2008.01.012.

Li, T., Dai, Z., Yu, M. and Zhang, W. (2021a), "Numerical investigation on the aerodynamic resistances of double-unit trains with different gap lengths", *Eng. Appl. Comput. Fluid Mech.*, **15**(1), 549-560. https://doi.org/10.1080/19942060.2021.1895321.

Li, X., Yang, H., Zhang, J., Qian, G., Yu, H. and Cai, J. (2021b), "Time-domain analysis of tamper displacement during dynamic compaction based on automatic control", *Coatings*, **11**(9), 1092. https://doi.org/10.3390/coatings11091092.

Liu, H., Liu, H. and Yang, J. (2018), "Vibration of FG magneto-electro-viscoelastic porous nanobeams on visco-Pasternak foundation", *Compos. Part B Eng.*, **155**, 244-256. https://doi.org/10.1016/j.compositesb.2018.08.042.

Liu, C., Gao, X., Chi, D., He, Y., Liang, M. and Wang, H. (2021), "On-line chatter detection in milling using fast kurtogram and frequency band power", *Eur. J. Mech. A Solid*, 104341. https://doi.org/10.1016/j.euromechsol.2021.104341.

Liu, X., Zhang, G., Li, J., Shi, G., Zhou, M., Huang, B., and Yang, W. (2020), "Deep learning for Feynman's path integral in strong-field time-dependent dynamics", *Phys. Rev. Lett.*, **124**(11), 113202. https://doi.org/10.1103/PhysRevLett.124.113202.

Mirjavadi, S.S., Forsat, M., Badnava, S. and Barati, M.R. (2020a), "Analyzing nonlocal nonlinear vibrations of two-phase geometrically imperfect piezo-magnetic beams considering piezoelectric reinforcement scheme", *J. Strain Anal. Eng. Des.*, **55**(7-8), 258-270. https://doi.org/10.1177%2F0309324720917285.

Mirjavadi, S.S., Forsat, M., Badnava, S., Barati, M.R. and Hamouda, A.M.S. (2020b), "Nonlinear dynamic characteristics of nonlocal multi-phase magneto-electro-elastic nano-tubes with different piezoelectric constituents", *Appl. Phys. A*, **126**(8), 1-16. https://doi.org/10.1007/s00339-020-03743-8.

Mirjavadi, S.S., Bayani, H., Khoshtinat, N., Forsat, M., Barati, M. R. and Hamouda, A.M.S. (2020c), "On nonlinear vibration behavior of piezo-magnetic doubly-curved nanoshells", *Smart Struct. Syst.*, **26**(5), 631-640. https://doi.org/10.12989/sss.2020.26.5.631.

Mirjavadi, S.S., Forsat, M., Yahya, Y.Z., Barati, M.R., Jayasimha, A.N. and Hamouda, A.M.S. (2020d), "Porosity effects on post-buckling behavior of geometrically imperfect metal foam doubly-curved shells with stiffeners", *Struct. Eng. Mech.*, **75**(6), 701-711. https://doi.org/10.12989/sem.2020.75.6.701.

Mirjavadi, S.S., Forsat, M., Mollaee, S., Barati, M.R., Afshari, B.M. and Hamouda, A.M.S. (2020e), "Post-buckling analysis of geometrically imperfect nanoparticle reinforced annular sector plates under radial compression", *Comput. Concrete*, **26**(1), 21-30. https://doi.org/10.12989/cac.2020.26.1.021.

Mirjavadi, S.S., Nikookar, M., Mollaee, S., Forsat, M., Barati, M.R. and Hamouda, A.M.S. (2020f), "Analyzing exact nonlinear forced vibrations of two-phase magneto-electro-elastic nanobeams under an elliptic-type force", *Adv. Nano Res.*, **9**(1), 47-58. https://doi.org/10.12989/anr.2020.9.1.047.

Mirjavadi, S.S., Forsat, M., Barati, M.R. and Hamouda, A.M.S. (2020g), "Investigating nonlinear forced vibration behavior of multi-phase nanocomposite annular sector plates using Jacobi elliptic functions", *Steel Compos. Struct.*, **36**(1), 87-101. https://doi.org/10.12989/scs.2020.36.1.087.

Mirjavadi, S.S., Forsat, M., Barati, M.R. and Hamouda, A.M.S. (2020h), "Post-buckling analysis of geometrically imperfect tapered curved micro-panels made of graphene oxide powder reinforced composite", *Steel Compos. Struct.*, **36**(1), 63-74. https://doi.org/10.12989/scs.2020.36.1.063.

Mirjavadi, S.S., Forsat, M., Barati, M.R. and Hamouda, A.M.S. (2020i), "Assessment of transient vibrations of graphene oxide reinforced plates under pulse loads using finite strip method", *Comput. Concrete*, **25**(6), 575-585. https://doi.org/10.12989/cac.2020.25.6.575.

Mirjavadi, S.S., Forsat, M., Barati, M.R. and Hamouda, A.M.S. (2020j), "Post-buckling of higher-order stiffened metal foam curved shells with porosity distributions and geometrical imperfection", *Steel Compos. Struct.*, **35**(4), 567-578. https://doi.org/10.12989/scs.2020.35.4.567.

Mirjavadi, S.S., Forsat, M., Yahya, Y.Z., Barati, M.R., Jayasimha, A.N. and Khan, I. (2020k), "Analysis of post-buckling of higher-order graphene oxide reinforced concrete plates with geometrical imperfection", *Adv. Concrete Constr.*, **9**(4), 397-406. https://doi.org/10.12989/acc.2020.9.4.397.

Muhammad, A.K., Hamad, L.B., Fenjan, R.M. and Faleh, N.M. (2019), "Analyzing large-amplitude vibration of nonlocal beams made of different piezo-electric materials in thermal environment", *Adv. Mater. Res.*, **8**(3), 237-257. https://doi.org/10.12989/amr.2019.8.3.237.

Pan, E. and Han, F. (2005), "Exact solution for functionally graded and layered magneto-electro-elastic plates", *Int. J. Eng. Sci.*, **43**(3-4), 321-339. https://doi.org/10.1016/j.ijengsci.2004.09.006.

Raheef, K.M., Ahmed, R.A., Nayeeif, A.A., Fenjan, R.M. and Faleh, N.M. (2021), "Analyzing dynamic response of nonlocal strain gradient porous beams under moving load and thermal environment", *Geomech. Eng.*, **26**(1), 89-99. https://doi.org/10.12989/gae.2021.26.1.089.

Shariati, A., Barati, M.R., Ebrahimi, F., Singhal, A. and Toghroli, A. (2020a), "Investigating vibrational behavior of graphene

sheets under linearly varying in-plane bending load based on the nonlocal strain gradient theory", *Adv*. *Nano Res*., **8**(4), 265-276. https://doi.org/10.12989/anr.2020.8.4.265.

Shariati, A., Barati, M.R., Ebrahimi, F. and Toghroli, A. (2020b), "Investigation of microstructure and surface effects on vibrational characteristics of nanobeams based on nonlocal couple stress theory", *Adv*. *Nano Res*, **8**(3), 191-202. https://doi.org/10.12989/anr.2020.8.3.191.

Thai, H.T. and Vo, T.P. (2012), "A nonlocal sinusoidal shear deformation beam theory with application to bending, buckling, and vibration of nanobeams", *Int*. *J*. *Eng*. *Sci*., **54**, 58-66. https://doi.org/10.1016/j.ijengsci.2012.01.009.

Xu, K.D., Guo, Y.J., Yang, Q., Zhang, Y.L., Deng, X., Zhang, A. and Chen, Q. (2021), "On-chip GaAs-based spoof surface plasmon polaritons at millimeter-wave regime", *IEEE Photo*. *Tech*. *L*., **33**(5), 255-258. https://doi.org/10.1109/LPT.2021.3054962.

Yang, W., Lin, Y., Chen, X., Xu, Y., Zhang, H., Ciappina, M. and Song, X. (2021), "Wave mixing and high-harmonic generation enhancement by a two-color field driven dielectric metasurface", *Chinese Opt*. *Lett*., **19**(12), 123202. https://doi.org/10.3788/COL202119.123202.

Zhang, X., Tang, Y., Zhang, F. and Lee, C.S. (2016), "A novel aluminum–graphite dual-ion battery", *Adv*. *Energy Mater*., **6**(11), 1502588. https://doi.org/10.1002/aenm.201502588.

Zhang, Z., Yang, F., Zhang, H., Zhang, T., Wang, H., Xu, Y. and Ma, Q. (2021), "Influence of CeO_2 addition on forming quality and microstructure of TiCx-reinforced CrTi4-based laser cladding composite coating", *Mater*. *Charact*., **171**, 110732. https://doi.org/10.1016/j.matchar.2020.110732.

Zhao, X., Zhu, W.D. and Li, Y.H. (2020a), "Analytical solutions of nonlocal coupled thermoelastic forced vibrations of micro-/nano-beams by means of Green's functions", *J*. *Sound Vib*., **481**, 115407. https://doi.org/10.1016/j.jsv.2020.115407.

AT